RSC Advances

PAPER

View Article Online
View Journal | View Issue

Cite this: *RSC Adv.*, 2019, **9**, 35904

Discovery of dihydrooxazolo[2,3-*a*]isoquinoliniums as highly specific inhibitors of hCE2†

Lixia Ding,‡[ac] Lu Wang,‡[b] Kun Zou,‡[a] Bo Li,*[ad] Yunqing Song,[b] Qihua Zhang,[a] Yitian Zhao,[b] Zhijian Xu,[ad] Guangbo Ge,*[b] Bo Zhao*[c] and Weiliang Zhu*[ade]

Received 16th September 2019
Accepted 28th October 2019

DOI: 10.1039/c9ra07457k

rsc.li/rsc-advances

Human carboxylesterase 2 (hCE2) is one of the most abundant esterases distributed in human small intestine and colon, which participates in the hydrolysis of a variety of ester-bearing drugs and thereby affects the efficacy of these drugs. Herein, a new compound (**23o**) with a novel skeleton of dihydrooxazolo[2,3-*a*]isoquinolinium has been discovered with strong inhibition on hCE2 (IC_{50} = 1.19 μM, K_i = 0.84 μM) and more than 83.89 fold selectivity over hCE1 (IC_{50} > 100 μM). Furthermore, **23o** can inhibit hCE2 activity in living HepG2 cells with the IC_{50} value of 2.29 μM, indicating that this compound has remarkable cell-membrane permeability and is capable for inhibiting intracellular hCE2. The SAR (structure–activity relationship) analysis and molecular docking results demonstrate that the novel skeleton of oxazolinium is essential for hCEs inhibitory activity and the benzyloxy moiety mainly contributes to the selectivity of hCE2 over hCE1.

Introduction

Mammalian carboxylesterases (CEs), important members of the serine hydrolase superfamily widely distributed in the lumen of endoplasmic reticulum in various tissues, are responsible for the hydrolysis of a wide range of endogenous and xenobiotic substrates containing ester, amides, thioesters and carbamates.[1–3] In human body, hCE1 and hCE2 are the main carboxylesterases, both of which play crucial roles in endo- and xenobiotic metabolism. As one of the most abundant esterases distributed in human small intestine and colon, hCE2 participates in hydrolysis of the ester-bearing drugs (such as irinotecan, prasugrel, capecitabine, flutamide) and thereby affects the efficacy of these drugs.[4–7] For instance, CPT-11 (irinotecan), an anticancer prodrug, exhibits strong anti-colorectal cancer activity by releasing the effective substance SN-38. However, excessive accumulation of SN-38 in the intestinal mucosa leads to delayed-onset diarrhoea even death.[8–10] To improve the potential clinical risk of these drugs, some highly specific hCE2 inhibitors have been used in clinical to reduce the local exposure of SN-38 in the intestinal mucosa, thereby ameliorating the intestinal toxicity of CPT-11.[11,12] Over the past decade, a wide variety of hCE2 inhibitors have been reported, including the natural triterpenoids,[13,14] flavonoids,[13–15] 1,2-diones[16,17] and *etc.* Although many compounds with strong hCE2 inhibitory activities have already been developed, the potent and specific inhibitors targeting intracellular hCE2 are still rarely reported.

DCZ0358 (Fig. 1) is a novel dihydrooxazolo[2,3-*a*]isoquinolinium discovered in the synthesis of berberine analogues.[18–20] Preliminary screening indicated that **DCZ0358** could effectively inhibit the catalytic activity of both hCE1 (IC_{50} = 4.04 μM) and hCE2 (IC_{50} = 16.03 μM), while its hydrolyzate **23b** showed a significant reduction of the inhibitory activity (hCE1 IC_{50} = 36.80 μM; hCE2 IC_{50} = 41.75 μM), which demonstrated that the oxazolinium moiety of **DCZ0358** is essential for the CE_S inhibitory activity (Fig. 1). In the synthesis of derivatives of **DCZ0358**, we have found that in addition to compound **23d** (Fig. 2), other compounds with modification of the substituents on the A and D rings cause structural instability

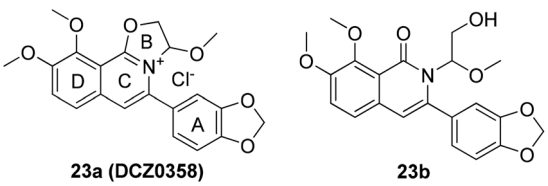

23a (DCZ0358) **23b**

Fig. 1 Structures of **23a** (DCZ0358) and **23b**.

[a]*Key Laboratory of Receptor Research, Drug Discovery and Design Center, Shanghai Institute of Materia Medica, Chinese Academy of Sciences, 555 Zuchongzhi Road, Shanghai 201203, China. E-mail: boli@simm.ac.cn; wlzhu@simm.ac.cn*

[b]*Shanghai University of Traditional Chinese Medicine, 1200 Cailun Road, Shanghai 201203, China. E-mail: geguangbo@dicp.ac.cn*

[c]*College of Chemistry and Materials Science, Nanjing Normal University, 1 Wenyuan Road, Nanjing 210097, China. E-mail: zhaobo@njnu.edu.cn*

[d]*University of Chinese Academy of Sciences, No. 19A Yuquan Road, Beijing 100049, China*

[e]*Open Studio for Druggability Research of Marine Natural Products, Pilot National Laboratory for Marine Science and Technology (Qingdao), 1 Wenhai Road, Aoshanwei, Jimo, Qingdao, 266237, China*

† Electronic supplementary information (ESI) available. See DOI: 10.1039/c9ra07457k

‡ These authors made equal contributions to this work.

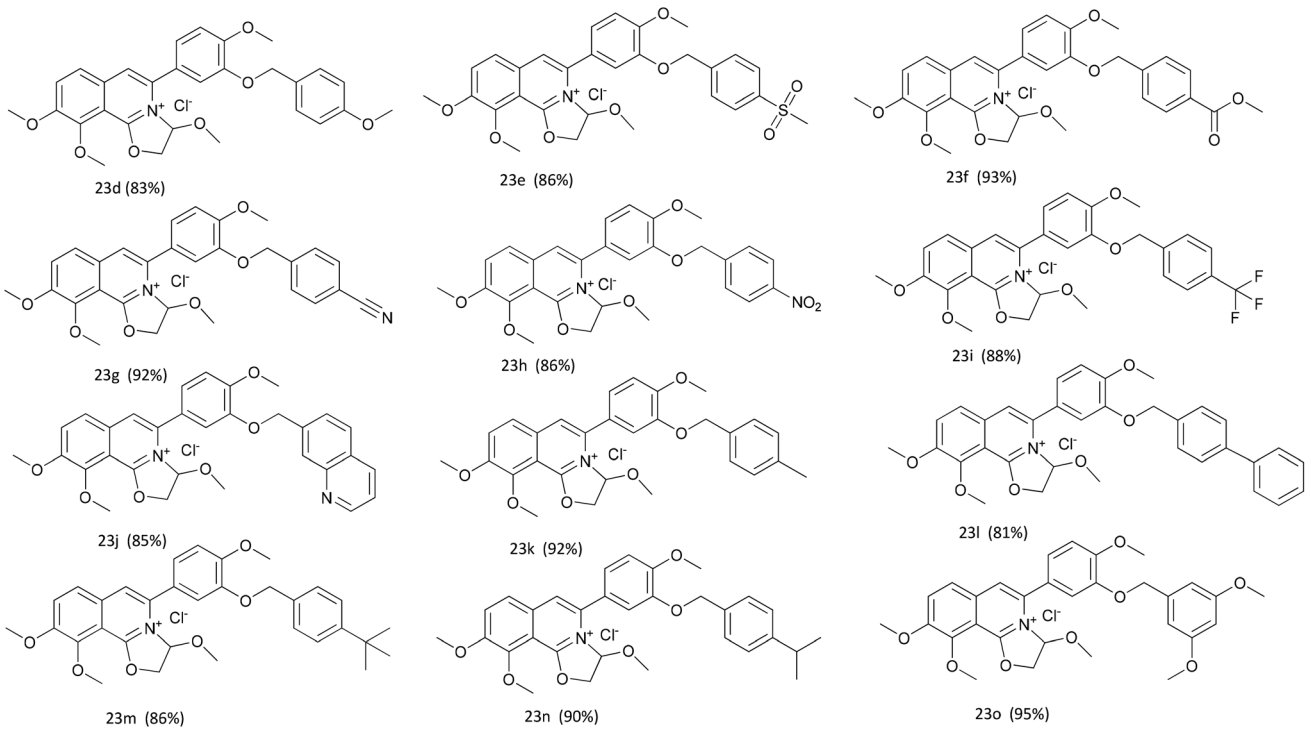

Fig. 2 The structures of compounds **23d–o**.

of the quaternary ammonium salt. Moreover, the bioactivity and selectivity of **23d** were improved (for hCE2 $IC_{50} = 6.889$ μM with >14.52-fold selectivity over hCE1). These results encouraged us to make further investigation of the structure–inhibition relationships of these berberine analogues as CEs inhibitors.

The previously reported synthetic route of **DCZ0358** is inconvenient to prepare more derivatives because of the harsh reaction conditions (Scheme 1).[21] Therefore, we designed a new synthetic route using compound **12** as the key intermediate (Scheme 2). Among the obtained new analogues, **23o** showed the highest selectivity and the best inhibitory activity (hCE1 IC_{50} > 100 μM; hCE2 $IC_{50} = 1.192$ μM, $K_i = 0.84$ μM). It was also found that **23o** could inhibit hCE2 activity in living HepG2 cells with the IC_{50} value of 2.29 μM, suggesting that the compound has remarkable cell-membrane permeability and is capable for inhibiting intracellular hCE2. Further molecular docking results showed that the methoxyl group at the benzyloxy ring of **23o** could tightly bind to the catalytic amino acid Ser-228 *via* H-bonding, which may account for the high selectivity of **23o** on hCE2 over hCE1.

Results and discussion

Synthetic procedures

Previously, we reported the synthetic route of **DCZ0358** (Scheme 1).[21] However, the application of *n*-butyl lithium reagent and low temperature condition (−78 °C) restricted the synthesis of derivatives. Therefore, developing a feasible route is important

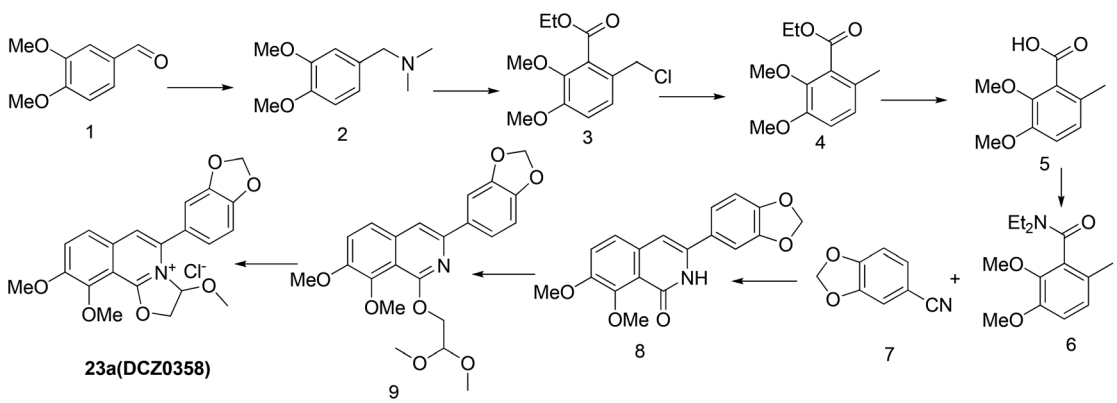

Scheme 1 The original synthetic route.

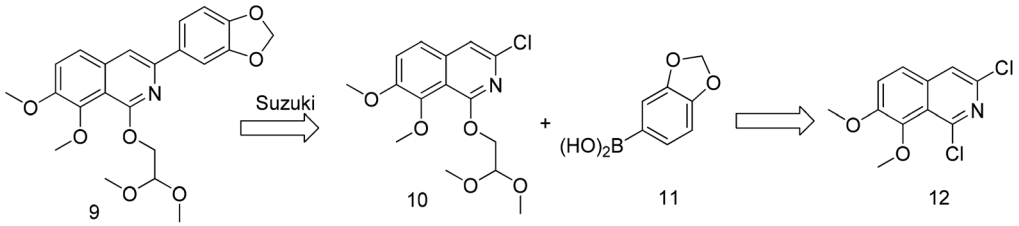

Scheme 2 The retrosynthetic analysis.

for the further medicinal chemistry research. Based on the retrosynthetic analysis (Scheme 1), compound **9** could be synthesized *via* Suzuki coupling reaction from **10** and **11**. Compound **10** could be smoothly prepared from the key intermediate **12**.

Firstly, 6,7-dimethoxy-1-indanone **13** was adopted as the starting material (Scheme 3). After oximation of **13** with *tert*-butyl nitrite under acidic condition, ketoxime **14** was obtained through filtration.[22–24] Subsequently, compound **14** was hydrolyzed by sodium hydroxide, and then dehydrated by *p*-toluenesulfonyl chloride to give benzonitrile **15**.[24] Finally, **15** was cyclized and chloridized by PCl_5 to provide the dichloroisoquinoline **12**.[24] However, the starting material **13** is very expensive and difficult to be prepared, which promoted us searching for alternative synthetic route.

Thus, we developed another route taking commercially available 3,4-dimethoxybenzaldehyde **1** as the starting material (Scheme 4). Compound **1** reacted with DMF and formic acid to afford tertiary amine **2** in 75% yield.[25] Then we added chloroformate to the mixture of **2** and *n*-butyl lithium under −78 °C to produce **16** in 80% yield.[26,27] Next, compound **16** was attracted by electrophilic reagent TMSCN to afford **17** (82% yield).[28] The operation for the hydrolysis of the methyl ester compound **17** to the compound **15** is difficult to be control. Subsequently, both ester and cyano groups were hydrolyzed to carboxyl groups under strong alkaline condition to give **18** (76% yield). Compound **18** was easily dehydrated in the presence of acetyl chloride to obtain compound **19** in 78% yield.[29] However, compound **20** was rather difficult to achieve from compound **18** or compound **19**. After trying various amines, we found that only ammonium carbonate could react with **19**.[30] However, this reaction occurred at a high temperature (280 °C) and gave a very low yield (22% yield) of **20**. Thus, compound **17** was directly reacted with sodium methoxide to afford compound **21** in 51% yield, followed by demethylation to produce dihydroisoquinoline-1,3-dione **20** with a high yield of 93%.[31] In order to convert **20** to the key intermediate **12**, we explored many reagents, such as PCl_5, $POCl_3$, $SOCl_2$ and $PhPOCl_2$, it turned out that $PhPOCl_2$ behaved the best yield with 47%.[31]

The key intermediate **12** reacted smoothly with hydroxyacetal under alkaline conditions to give compound **10** with high yield (98%),[32] and then **10** reacted with various arylboronic acids containing a benzyloxy structure to produce **22** in yields ranging from 46% to 98%.[19] Finally **22** were cyclized under acidic conditions to give a series of dihydrooxazolo[2,3-*a*]isoquinolinium analogues (Scheme 5, compounds **23d–23o** in Fig. 2). The present synthetic route is convenient to scale up and benefits further pharmaceutical research.

Biological activity assays

We designed and synthesized more than 30 derivatives of **DCZ0358**. However, the five-ring quaternary ammonium component of some derivatives was unstable to decompose easily into its hydrolyzate **23b**. With 12 stable compounds in hand, we conducted experiments to assay inhibitory activities against both hCE1 and hCE2 using a panel of fluorescent probe substrates.[33–36] D-Luciferin methyl ester (DME) was used as a probe substrate, and nevadensin (a specific hCE1 inhibitor) was used as a positive inhibitor control for hCE1. Fluorescein diacetate (FD) was used as a specific probe substrate, and loperamide (LPA) was used as a positive inhibitor control of hCE2. The IC_{50} values of all derivatives were evaluated and listed in Table 1.

Table 1 showed that the inhibitory effects of these compounds against hCE2 were enhanced significantly when the methylenedioxy group on A ring was changed into benzyloxy group. The IC_{50} values of **23n** (hCE2 IC_{50} 1.66 ± 0.21 μM) and **23o** (hCE2 IC_{50} 1.19 ± 0.10 μM) were improved more than tenfold comparing to that of **23a** (hCE2 IC_{50} 16.03 ± 1.49 μM). However, different types of the substituents on the A ring didn't have significant effects on the inhibitory activities, *e.g.*, **23k** (hCE2 IC_{50} 5.58 ± 0.94 μM), **23l** (hCE2 IC_{50} 2.64 ± 0.45 μM), **23m** (hCE2 IC_{50} 2.33 ± 0.20 μM), **23n** (hCE2 IC_{50} 1.66 ± 0.21 μM) and **23o** (hCE2 IC_{50} 1.19 ± 0.10 μM)

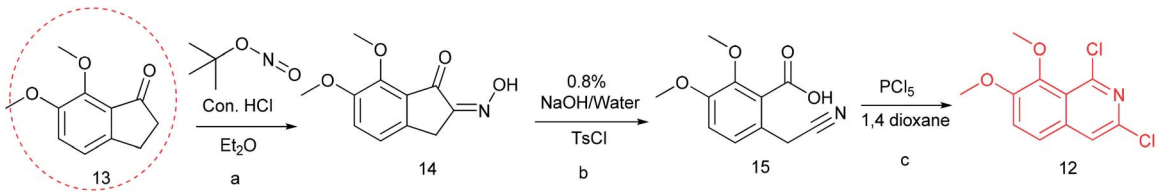

Scheme 3 The synthesis of compound **12**. Reagents and conditions: (a) *tert*-butyl nitrite, HCl (cat.), diethyl ether, r.t., 2 h; (b) NaOH (8%), 50 °C; TosCl, 80 °C, 3 h; (c) PCl_5, 1,4-dioxane, 90 °C, 12 h.

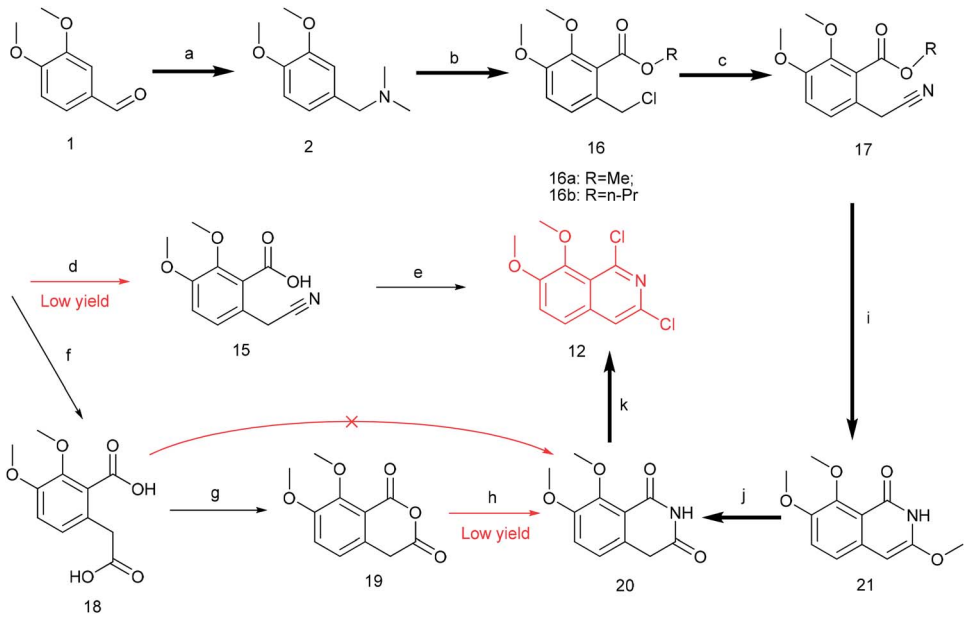

Scheme 4 The synthesis of compound **12**. Reagents and conditions: (a) DMF, HCOOH, 150 °C, 5 h; (b) *n*-BuLi (0 °C), $ClCOOCH_3$/$ClCOOC_3H_7$ (−78 °C), dry THF, r.t 12 h; (c) TMSCN, TBAF, MeCN, 80 °C 12 h; (d) NaOH (2.9 M), 1,4-dioxane, 40 °C, 3 h; (e) PCl_5, 1,4-dioxane, 90 °C, 12 h; (f) NaOH (10 M), 1,4-dioxane, 90 °C, 8 h; (g) AcCl, 50 °C, 2 h; (h) $(NH_4)_2CO_3$, 280 °C, 2 h; (i) MeONa, dry MeOH, 80 °C 1 h; (j) MeOH, HCl (3 M), 100 °C 1 h; (k) $PhPOCl_2$, 160 °C, 3 h.

with electron-donating groups on the benzyloxy ring were similar to that of **23e** (hCE2 IC_{50} 11.46 ± 1.76 μM), **23f** (hCE2 IC_{50} 5.73 ± 0.79 μM) and **23h** (hCE2 IC_{50} 3.32 ± 0.87 μM) with electron-withdrawing groups. In terms of the selectivity, it improved apparently according to the values of IC_{50} (hCE2)/IC_{50} (hCE1) shown in Table 1. For instance, the value of IC_{50} (hCE2)/IC_{50} (hCE1) of **23o** was up to 83 while that of **23a** was only 0.25. Thus, **23o** have the best selectivity on hCES2 among all these newly synthesized compounds.

Collectively, the structure–activity relationships of these compounds were summarized as follows, (1) the oxazolinium moiety is crucial for the inhibitory activity against hCEs; (2) the benzyloxy group on the A ring mainly contributed to the selectivity of hCE2 over hCE1 (Fig. 3).

The inhibition kinetic of **23o** against hCE2-mediated FD hydrolysis has been carefully investigated and the results showed that **23o** functioned as a mixed inhibitor against hCE2-mediated FD hydrolysis, with the K_i value of 0.84 μM (Fig. 4B). Furthermore, in view of that hCE2 is an intracellular enzyme, the inhibition potential of **23o** was also investigated. As shown in Fig. 5, **23o** could strongly inhibit intracellular hCE2-mediated NCEN hydrolysis and reduce the fluorescence intensity in the green channel (for the hydrolytic metabolite of NCEN) in living HepG2 cells *via* a dose-dependent manner. Meanwhile, the IC_{50}

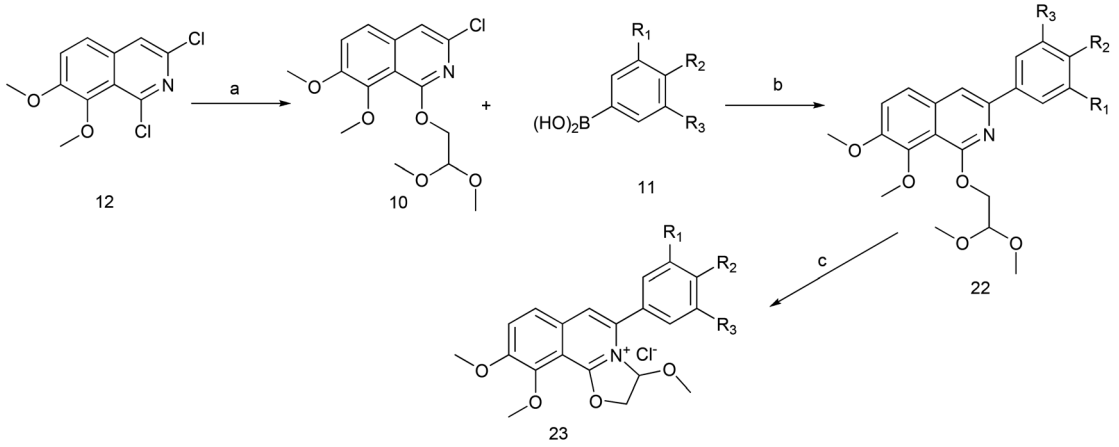

Scheme 5 The synthesis of **DCZ0358** analogues. Reagents and conditions: (a) NaH, glycolaldehyde dimethyl acetal, THF, r.t.12 h; (b) $Pd_2(dba)_3$, Xphos, K_3PO_4, 1,4-dioxane, 90 °C, 12 h; (c) acetone, HCl–Et_2O (5 : 1), r.t. 1 h.

Table 1 The IC_{50} values of **DCZ0358** and its derivatives on hCE1 and hCE2[a]

Compound	IC_{50} (μM) for hCE1	IC_{50} (μM) for hCE2	Selectivity IC_{50}(hCE2)/IC_{50}(hCE1)
23a	4.04 ± 0.40	16.03 ± 1.49	>0.25
23b	36.80 ± 7.70	41.75 ± 18.15	>0.88
23c	>100	6.89 ± 1.09	>14.52
23e	>100	11.46 ± 1.76	>8.72
23f	>100	5.73 ± 0.79	>17.46
23g	>100	3.33 ± 0.32	>30.07
23h	>100	3.32 ± 0.87	>30.14
23i	>100	2.43 ± 0.28	>41.22
23j	>100	3.77 ± 0.25	>26.51
23k	>100	5.58 ± 0.94	>17.94
23l	>100	2.64 ± 0.45	>37.89
23m	>100	2.33 ± 0.20	>42.81
23n	>100	1.66 ± 0.21	>60.31
23o[a]	>100	1.19 ± 0.10	>83.89
Nevadensin[b]	2.64 ± 0.22	—	—
LPA[c]	—	6.24 ± 0.93	—

[a] Inhibition potential of all compounds were investigated in living HepG2 cells. [b] Nevadensin was used as a positive inhibitor of hCE1. [c] LPA was used as a positive inhibitor of hCE2.

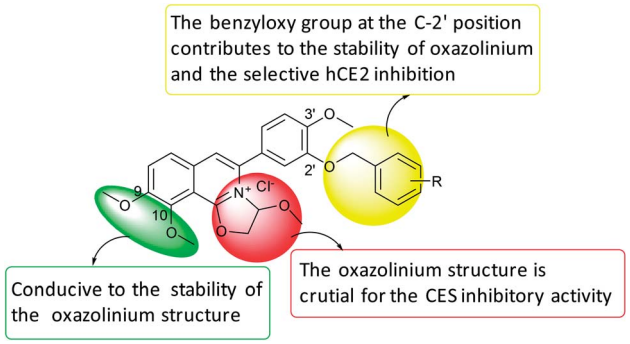

Fig. 3 SAR summary of **DCZ0358** analogues.

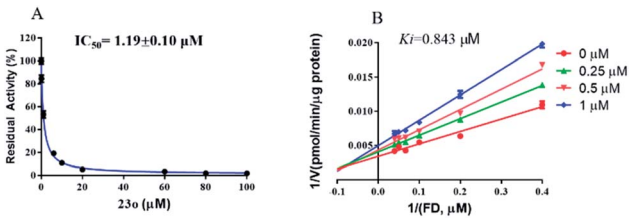

Fig. 4 The dose-dependent inhibition curve of **23o** (A) and the Lineweaver–Burk plots of **23o** against hCE2-mediated FD hydrolysis (B).

value of **23o** against intracellular hCE2 was also evaluated as 2.29 μM (Fig. S2B†).

Molecular docking

In order to investigate the interaction mechanism of **23o** with hCE2, molecular docking of **23o** to the active site of hCE2 was performed. As shown in Fig. 6, there are hydrogen bond between the methoxyl of ring D with Arg-355 (3.16 Å), and a T-type π–π interaction between the ring D with the Arg-355, as well as, hydrogen bond between the oxygen atom of ring B with Phe-307 (3.17 Å) in the entrance of the active cavity of hCE2. These interactions facilitate the entry of **23o** into the active cavity of hCE2. However, the hydrolysate of **23o** cannot enter the active cavity of hCE2, due to its small inlet. In addition, the methoxyl group at the benzyloxy end of **23o** could tightly bind to the catalytic amino acid Ser-228 (1.6 Å) *via* strong H-bonding, as well as, with Ala-150 (3.18 Å), and there are strong hydrophobic interactions between the benzyloxy group of **23o** with the key residues in the active cavity of hCE2. These interactions may account for the high selectivity of **23o** on hCE2. The strong H-bond interaction between **23o** and Ser-228 indicates that **23o** may obstruct hCE2-mediated hydrolysis, possibly because Ser-

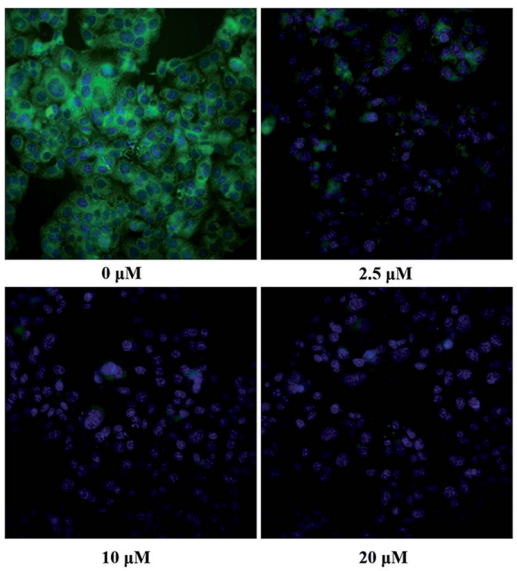

Fig. 5 The images of HepG2 cells stained with NCEN (10 μM) and Hoechst 33342 (1 μM) at 37 °C for 50 min in the presence of **23o** at various concentrations (0 μM, 2.5 μM, 10 μM and 20 μM). All data was shown as mean ± SD.

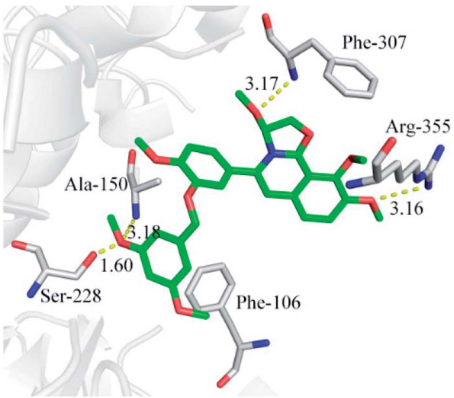

Fig. 6 Molecular docking indicates the interactions between compound **23o** and hCE2.

228 is an important residue involved in substrate recognition and catalysis of hCE2. These findings agreed well with the experimental data where **23o** exhibited much more potent inhibitory effect on hCE2 but a relatively weaker one on hCE1.

Conclusions

A new compound **23o** with a novel skeleton of dihydrooxazolo [2,3-*a*]isoquinolinium was discovered with good inhibitory activity on hCE2 (IC_{50} = 1.19 μM, K_i = 0.84 μM) and high selectivity over hCE1 (IC_{50} > 100 μM). The SAR (structure–activity relationship) analysis and molecular docking results revealed that the novel oxazolinium moiety is essential for hCE2 inhibitory activity, while the benzyloxy moiety contributes to the selectivity of hCE2 over hCE1. Furthermore, **23o** could strongly inhibit intracellular hCE2 in living HepG2 cells, with the IC_{50} value of 2.29 μM. These findings are important for further research and development of hCE2 inhibitors with high specificity and efficacy.

Experimental

Chemical synthesis

Materials. All starting materials were obtained from commercial suppliers and used without further purification. The ^{1}H and ^{13}C NMR spectra were taken on Bruker Avance-600 or 500 or 400, Varian MERCURY Plus-400 or 300 NMR spectrometer operating at 400 MHz or 300 MHz for ^{1}H NMR, 125 MHz or 100 MHz for ^{13}C NMR, using TMS as internal standard and $CDCl_3$ or methanol-d_4 or DMSO-d_6 as solvent.^{13}C NMR spectra were recorded with complete proton decoupling. The ESI-MS or EI-MS was recorded on Finnigan LCQ/DECA or Thermo-DFS, respectively. The HRMS were obtained from Micromass Ultra Q-TOF (ESI) or Thermo-DFS (EI) spectrometer. Flash column chromatography was carried out using silica gel (200–400 mesh). Thin layer chromatography (TLC) was used silica gel F254 fluorescent treated silica that were visualised under UV light (254 nm).

Synthetic procedure. Compounds **DCZ0358** and **23b** have been reported in our previous work.[18,20] Synthesis of 3,9,10-trimethoxy-5-(4-methoxy-3-((4-methoxybenzyl)oxy)phenyl)-2,3-dihydrooxazolo[2,3-*a*]isoquinolin-4-ium (**23d**). To a solution of **22d** (56 mg, 0.1 mmol) in acetone (5 mL) was added hydrochloric acid (1 mL, 2.0 M in diethyl ether), and then the mixture was stirred for 2 h at room temperature. The solution was evaporated *in vacuo* to obtain the titled compound **23d** as yellow solid (46 mg, 83%). ^{1}H NMR (500 MHz, DMSO-d_6) δ 8.15 (s, 1H), 7.99 (s, 1H), 7.81 (s, 1H), 7.34 (s, 2H), 7.13 (s, 3H), 6.91 (s, 2H), 6.62 (s, 1H), 5.30 (s, 1H), 5.20 (s, 1H), 4.69 (s, 2H), 4.02 (s, 3H), 3.95 (s, 3H), 3.85 (s, 3H), 3.73 (s, 3H), 2.95 (s, 3H). ^{13}C NMR (125 MHz, DMSO-d_6) δ 161.2, 159.7, 152.9, 149.9, 147.3, 146.2, 136.8, 134.5, 130.9, 130.1, 126.1, 124.9, 124.5, 120.9, 118.8, 116.5, 114.5, 112.8, 110.6, 90.9, 76.5, 62.3, 57.5, 56.3, 55.8, 55.7, 46.8. HRMS (EI) calcd for $C_{30}H_{17}O_7N$ 503.1000 $[M]^+$, found 503.0990.

3,9,10-Trimethoxy-5-(4-methoxy-3-((4-(methylsulfonyl)benzyl) oxy)phenyl)-2,3-dihydrooxazolo[2,3-a]isoquinolin-4-ium ***(23e).*** Compound **23e** was prepared from compound **22e** (58 mg, 0.1 mmol) as a yellow solid (48 mg, 86%). ^{1}H NMR (400 MHz, DMSO-d_6) δ 8.18 (d, J = 7.6 Hz, 1H), 7.97 (d, J = 7.2 Hz, 3H), 7.87 (s, 1H), 7.73 (s, 2H), 7.44 (s, 1H), 7.32 (s, 1H), 7.26 (s, 1H), 6.62 (s, 1H), 5.33 (m, 4H), 4.13–3.82 (m, 9H), 3.22 (s, 3H), 2.85 (s, 3H). ^{13}C NMR (125 MHz, DMSO-d_6) δ 161.1, 153.0, 151.3, 147.9, 146.2, 143.2, 140.8, 136.4, 134.4, 128.7, 127.7, 126.2, 124.9, 124.3, 123.3, 119.1, 114.9, 112.9, 110.5, 91.0, 76.4, 69.8, 62.3, 57.5, 56.4, 55.8, 44.0. HRMS (EI) calcd for $C_{29}H_{29}O_8NS$ 551.1608 $[M]^+$, found 551.1607.

3,9,10-Trimethoxy-5-(4-methoxy-3-((4-(methoxycarbonyl)benzyl) oxy)phenyl)-2,3-dihydrooxazolo[2,3-a]isoquinolin-4-ium ***(23f).*** Compound **23f** was prepared from compound **22f** (56 mg, 0.1 mmol) as a yellow solid (50 mg, 93%). ^{1}H NMR (600 MHz, $CDCl_3$) δ 8.17 (d, J = 8.9 Hz, 2H), 8.01 (s, 2H), 7.99 (s, 1H), 7.86 (s, 1H), 7.61 (d, J = 7.8 Hz, 2H), 7.42 (s, 1H), 7.32 (m, 1H), 7.25 (d, J = 8.4 Hz, 1H), 6.61 (d, J = 6.0 Hz, 1H), 5.33 (m, 2H), 5.27 (m, 1H), 5.22 (m, 1H), 4.04 (s, 3H), 3.97 (s, 3H), 3.89 (s, 3H), 3.85 (s, 3H), 2.86 (s, 3H). ^{13}C NMR (125 MHz, DMSO-d_6) δ 166.5, 161.1, 153.0, 151.3, 148.0, 146.2, 142.7, 136.4, 134.4, 129.8, 129.6, 128.1, 126.1, 124.9, 124.3, 123.2, 119.1, 114.9, 112.9, 110.6, 91.0, 76.4, 70.0, 62.3, 57.4, 56.4, 55.8, 52.7. HRMS (EI) calcd for $C_{30}H_{29}O_8N$ 531.1888 $[M]^+$, found 531.1882.

5-(3-((4-Cyanobenzyl)oxy)-4-methoxyphenyl)-3,9,10-trimethoxy-2,3-dihydrooxazolo[2,3-a]isoquinolin-4-ium ***(23g).*** Compound **23g** was prepared from compound **22g** (53 mg, 0.1 mmol) as a yellow solid (46 mg, 92%). ^{1}H NMR (600 MHz, DMSO-d_6) δ 8.17 (d, J = 9.0 Hz, 1H), 8.01 (d, J = 9.0 Hz, 1H), 7.90 (d, J = 4.2 Hz, 2H), 7.86 (s, 1H), 7.66 (d, J = 7.8 Hz, 2H), 7.43 (d, J = 1.8 Hz, 1H), 7.33 (dd, J = 8.4, 1.8 Hz, 1H), 7.26 (d, J = 7.8 Hz, 1H), 6.64 (d, J = 6.0 Hz, 1H), 5.34 (m, 2H), 5.29 (m, 1H), 5.24 (m, 1H), 4.05 (s, 3H), 3.98 (s, 3H), 3.90 (s, 3H), 2.87 (s, 3H). ^{13}C NMR (125 MHz, DMSO-d_6) δ 161.1, 153.0, 151.3, 147.8, 146.2, 143.0, 136.3, 134.4, 133.0, 128.6, 126.1, 124.9, 124.3, 123.3, 119.2, 119.1, 114.8, 112.9, 111.1, 110.6, 91.0, 76.4, 69.7, 62.3, 57.4, 56.4, 55.8. HRMS (EI) calcd for $C_{29}H_{26}O_6N_2$ 498.1785 $[M]^+$, found 498.1785.

3,9,10-Trimethoxy-5-(4-methoxy-3-((4-nitrobenzyl)oxy)phenyl)-2,3-dihydrooxazolo[2,3-a]isoquinolin-4-ium ***(23h).*** Compound **23h** was prepared from compound **22h** (55 mg, 0.1 mmol) as a yellow solid (45 mg, 86%). ^{1}H NMR (400 MHz, DMSO-d_6) δ 8.30 (d, J = 8.4 Hz, 2H), 8.19 (d, J = 9.2 Hz, 1H), 8.01 (d, J = 9.2 Hz,

1H), 7.87 (s, 1H), 7.74 (d, J = 8.4 Hz, 2H), 7.43 (s, 1H), 7.34 (d, J = 8.4 Hz, 1H), 7.28 (d, J = 8.4 Hz, 1H), 6.66 (d, J = 5.2 Hz, 1H), 5.44–5.35 (m, 2H), 5.34 (s, 1H), 5.23 (d, J = 6.4 Hz, 1H), 4.05 (s, 3H), 3.98 (s, 3H), 3.91 (s, 3H), 2.89 (s, 3H). ^{13}C NMR (125 MHz, DMSO-d_6) δ 160.6, 152.5, 150.8, 147.3, 147.1, 145.7, 144.6, 135.8, 133.9, 128.3, 125.7, 124.4, 123.8, 123.6, 122.9, 118.6, 114.4, 112.4, 110.1, 90.5, 75.9, 69.1, 61.8, 56.9, 55.9, 55.3. HRMS (EI) calcd for $C_{28}H_{26}O_8N_2$ 518.1684 $[M]^+$, found 518.1688.

3,9,10-Trimethoxy-5-(4-methoxy-3-((4-(trifluoromethyl)benzyl) oxy)phenyl)-2,3-dihydrooxazolo[2,3-a]isoquinolin-4-ium ***(23i).*** Compound **23i** was prepared from compound **22i** (57 mg, 0.1 mmol) as a yellow solid (48 mg, 88%). ^{1}H NMR (500 MHz, DMSO-d_6) δ 8.20 (d, J = 7.2 Hz, 1H), 8.03 (d, J = 6.8 Hz, 1H), 7.89 (s, 1H), 7.82 (d, J = 6.0 Hz, 2H), 7.72 (d, J = 6.4 Hz, 2H), 7.46 (s, 1H), 7.35 (d, J = 6.4 Hz, 1H), 7.28 (d, J = 6.4 Hz, 1H), 6.64 (s, 1H), 5.36 (m, 3H), 5.27 (s, 1H), 4.07 (s, 3H), 4.01 (s, 3H), 3.93 (s, 3H), 2.88 (s, 3H). ^{13}C NMR (125 MHz, DMSO-d_6) δ 160.6, 152.5, 150.8, 147.4, 145.7, 141.6, 135.9, 133.9, 128.1, 125.7, 125.4, 125.4, 124.4, 123.8, 122.7, 119.4, 118.6, 114.3, 112.4, 110.1, 90.5, 75.9, 69.3, 61.8, 56.9, 55.9, 55.3. HRMS (EI) calcd for $C_{29}H_{26}O_6NF_3$ 541.1707 $[M]^+$, found 541.1710.

3,9,10-Trimethoxy-5-(4-methoxy-3-(quinolin-7-ylmethoxy) phenyl)-2,3-dihydrooxazolo[2,3-a]isoquinolin-4-ium ***(23j).*** Compound **23j** was prepared from compound **22j** (58 mg, 0.1 mmol) as a yellow solid (45 mg, 85%). ^{1}H NMR (400 MHz, DMSO-d_6) δ 8.99 (s, 1H), 8.57 (d, J = 7.2 Hz, 1H), 8.18 (d, J = 8.0 Hz, 1H), 8.07 (d, J = 7.6 Hz, 1H), 8.00 (s, 2H), 7.89 (s, 1H), 7.73 (s, 1H), 7.70 (s, 1H), 7.57 (s, 1H), 7.32 (d, J = 5.6 Hz, 1H), 7.26 (d, J = 7.2 Hz, 1H), 6.74 (s, 1H), 5.91 (m, 1H), 5.82 (m, 1H), 5.34 (m, 1H), 5.23 (s, 1H), 4.04 (s, 3H), 3.96 (s, 3H), 3.89 (s, 3H), 2.93 (s, 3H). ^{13}C NMR (125 MHz, DMSO-d_6) δ 161.1, 153.0, 151.2, 150.0, 148.5, 146.2, 136.5, 134.5, 134.0, 129.8, 129.2, 128.7, 128.4, 127.3, 126.1, 125.0, 124.4, 122.9, 122.3, 119.1, 115.7, 114.3, 112.8, 110.6, 91.0, 76.5, 67.0, 62.3, 57.5, 56.4, 55.8. HRMS (EI) calcd for $C_{31}H_{28}O_6N_2$ 524.1942 $[M]^+$, found 524.1951.

3,9,10-Trimethoxy-5-(4-methoxy-3-((4-methylbenzyl)oxy) phenyl)-2,3-dihydrooxazolo[2,3-a]isoquinolin-4-ium ***(23k).*** Compound **23k** was prepared from compound **22k** (52 mg, 0.1 mmol) as a yellow solid (45 mg, 92%). ^{1}H NMR (400 MHz, DMSO-d_6) δ 8.16 (s, 1H), 7.99 (s, 1H), 7.85 (s, 1H), 7.39 (s, 1H), 7.33 (s, 2H), 7.26 (s, 1H), 7.20 (s, 3H), 6.54 (s, 1H), 5.31 (s, 1H), 5.13 (s, 3H), 4.02 (s, 3H), 3.95 (s, 3H), 3.85 (s, 3H), 2.82 (s, 3H), 2.28 (s, 3H). ^{13}C NMR (125 MHz, DMSO-d_6) δ 160.6, 152.4, 150.8, 147.6, 145.7, 137.3, 136.0, 133.9, 133.5, 129.0, 127.9, 125.7, 124.5, 123.7, 122.4, 118.5, 114.1, 112.3, 110.0, 90.5, 76.0, 70.0, 61.9, 57.1, 55.9, 55.4, 20.8. HRMS (EI) calcd for $C_{29}H_{29}O_6N$ 487.1989 $[M]^+$, found 487.1989.

5-(3-([1,1′-Biphenyl]-4-ylmethoxy)-4-methoxyphenyl)-3,9,10-trimethoxy-2,3-dihydrooxazolo[2,3-a]isoquinolin-4-ium ***(23l).*** Compound **23l** was prepared from compound **22l** (58 mg, 0.1 mmol) as a yellow solid (45 mg, 81%). ^{1}H NMR (500 MHz, DMSO-d_6) δ 8.20 (d, J = 6.8 Hz, 1H), 8.03 (d, J = 6.8 Hz, 1H), 7.90 (s, 1H), 7.74 (d, J = 6.0 Hz, 2H), 7.70 (d, J = 6.0 Hz, 2H), 7.58 (d, J = 6.0 Hz, 2H), 7.53–7.47 (m, 3H), 7.40 (t, J = 6.0 Hz, 1H), 7.33 (d, J = 6.4 Hz, 1H), 7.27 (d, J = 6.4 Hz, 1H), 6.63 (s, 1H), 5.34 (m, 1H), 5.27 (m, 3H), 4.07 (s, 3H), 4.00 (s, 3H), 3.93 (s, 3H), 2.88 (s, 3H). ^{13}C NMR (125 MHz, DMSO-d_6) δ 160.6, 152.5, 150.8, 147.7, 145.7, 139.9, 139.7, 136.0, 135.8, 133.9, 129.0, 128.4, 127.6, 126.8, 126.6, 125.7, 124.4, 123.8, 122.4, 118.6, 114.1, 112.3, 110.0, 90.5, 76.0, 69.8, 61.8, 57.0, 55.8, 55.4. HRMS (EI) calcd for $C_{34}H_{31}O_6N$ 549.2146 $[M]^+$, found 549.2146.

5-(3-((4-(tert-Butyl)benzyl)oxy)-4-methoxyphenyl)-3,9,10-trimethoxy-2,3-dihydrooxazolo[2,3-a]isoquinolin-4-ium ***(23m).*** Compound **23m** was prepared from compound **22m** (56 mg, 0.1 mmol) as a yellow solid (46 mg, 86%). ^{1}H NMR (500 MHz, DMSO-d_6) δ 8.18 (d, J = 7.2 Hz, 1H), 8.02 (d, J = 6.8 Hz, 1H), 7.88 (s, 1H), 7.44 (d, J = 5.6 Hz, 3H), 7.40 (d, J = 6.4 Hz, 2H), 7.30 (d, J = 6.8 Hz, 1H), 7.23 (d, J = 6.8 Hz, 1H), 6.56 (s, 1H), 5.32 (m, 1H), 5.26 (m, 1H), 5.17 (m, 2H), 4.05 (s, 3H), 3.99 (s, 3H), 3.88 (s, 3H), 2.82 (s, 3H), 1.29 (s, 9H). ^{13}C NMR (125 MHz, DMSO-d_6) δ 161.1, 153.0, 151.3, 151.1, 148.2, 146.2, 136.5, 134.5, 134.1, 128.3, 126.2, 125.7, 124.9, 124.3, 122.8, 119.0, 114.4, 112.7, 110.5, 91.0, 76.5, 70.3, 62.3, 57.5, 56.3, 55.9, 34.8, 31.6. HRMS (EI) calcd for $C_{32}H_{35}O_6N$ 529.2459 $[M]^+$, found 529.2459.

5-(3-((4-Isopropylbenzyl)oxy)-4-methoxyphenyl)-3,9,10-trimethoxy-2,3-dihydrooxazolo[2,3-a]isoquinolin-4-ium ***(23n).*** Compound **23n** was prepared from compound **22n** (55 mg, 0.1 mmol) as a yellow solid (50 mg, 90%).^{1}H NMR (600 MHz, DMSO-d_6) δ 8.18 (d, J = 6.0 Hz, 1H), 8.01 (d, J = 6.0 Hz, 1H), 7.87 (s, 1H), 7.43 (d, J = 1.2 Hz, 1H), 7.39 (d, J = 5.2 Hz, 2H), 7.31–7.27 (m, 3H), 7.22 (d, J = 5.6 Hz, 1H), 6.55 (d, J = 4.0 Hz, 1H), 5.31 (m, 1H), 5.24 (m, 1H), 5.18 (m, 1H), 5.13 (m, 1H), 4.05 (s, 3H), 3.98 (s, 3H), 3.87 (s, 3H), 2.94–2.85 (m, 1H), 2.82 (s, 3H), 1.20 (s, 3H), 1.19 (s, 3H). ^{13}C NMR (125 MHz, DMSO-d_6) δ 161.1, 153.0, 151.3, 148.8, 148.2, 146.2, 136.5, 134.5, 134.4, 128.5, 126.9, 126.1, 124.9, 124.3, 122.8, 119.0, 114.4, 112.7, 110.5, 91.0, 76.4, 70.4, 62.3, 57.4, 56.3, 55.9, 33.7, 24.3. HRMS (EI) calcd for $C_{31}H_{33}O_6N$ 515.2302 $[M]^+$, found 515.2295.

5-(3-((3,5-Dimethoxybenzyl)oxy)-4-methoxyphenyl)-3,9,10-trimethoxy-2,3-dihydrooxazolo[2,3-a]isoquinolin-4-ium ***(23o).*** Compound **23o** was prepared from compound **22o** (56 mg, 0.1 mmol) as a yellow solid (51 mg, 95%). ^{1}H NMR (500 MHz, DMSO-d_6) δ 8.18 (d, J = 8.5 Hz, 1H), 8.00 (d, J = 9.0 Hz, 1H), 7.87 (m, 1H), 7.39 (s, 1H), 7.32–7.26 (m, 1H), 7.24 (d, J = 8.5 Hz, 1H), 6.62 (s, 2H), 6.52 (s, 1H), 6.47 (s, 1H), 5.33 (m, 1H), 5.26–5.17 (m, 1H), 5.15 (s, 2H), 4.05 (s, 3H), 3.98 (s, 3H), 3.90 (s, 3H), 3.74 (s, 6H), 2.84 (s, 3H). ^{13}C NMR (125 MHz, DMSO-d_6) δ 161.1, 161.1, 153.0, 151.4, 148.0, 146.2, 139.5, 136.5, 134.4, 126.2, 124.9, 124.2, 123.0, 119.0, 114.7, 112.9, 110.5, 106.1, 99.8, 91.0, 76.4, 70.4, 62.3, 57.5, 56.4, 55.9, 55.7. HRMS (EI) calcd for $C_{30}H_{31}O_8N$ 533.2044 $[M]^+$, found 533.2031.

Biology

Materials. Fluorescein diacetate (FD) and loperamide (LPA) were purchased from TCI (Tokyo Japan), Luciferin Detection Reagent (LDR) was purchased from Promega Corporation (USA). *N*-(2-Butyl-1,3-dioxo-2,3-dihydro-1*H*-phenalen-6-yl)-2-chloroacetamide (NCEN) and D-luciferin methyl ester (DME) were synthesized by authors according to the previously reported synthetic scheme.[37,38] Nevadensin was purchased from Chengdu Preferred Biotech Co., Ltd. (Chengdu, China). Pooled human liver microsomes (HLMs, from 50 donors, lot no. X008067) were obtained from Bioreclamation IVT (Baltimore,

MD, USA) and stored at −80 °C until use. DMSO was purchased from fisher. Phosphate buffer was prepared using Millipore water and then stored at 4 °C until use. All tested compounds were solved by DMSO and stored at 4 °C until use. LC grade acetonitrile and DMSO (Tedia, USA) were used throughout.

hCE1 inhibition assay. DME was used as a probe substrate for evaluating the inhibitory effects of all DCZ0358 derivatives on hCE1, while nevadensin (a specific hCE1 inhibitor) was used as a positive control.[39] Briefly, 100 μL incubation mixture containing 91 μL PBS (pH 6.8), 2 μL inhibitor at different concentrations and 5 μL HLM (1 μg mL^{-1}, final concentration), were pre-incubated at 37 °C for 10 min. Subsequently, 2 μL DME (3 μM final concentration, close to the K_m value of DME in HLM) was added to initiate the reaction. After incubating for 10 min at 37 °C in a shaking bath, the reaction was stopped by the addition of LDR (100 μL). The microplate reader (SpectraMax® iD3, Molecular Devices, Austria) was used for luminescence measurements. The gain value of luminescence detection was set at 140 volts, and the integration time was set at 1 s. The chemical structure of DME and its hydrolytic metabolite (D-luciferin), as well as the detection conditions for D-luciferin are depicted in Table S1.† The negative control incubation (DMSO only) was carried out under the same conditions. The residual activity was calculated using the following formula, the residual activity (%) = (the florescence intensity in the presence of inhibitor)/the florescence intensity in negative control × 100%. The residual activities are show in Fig. S1.†

hCE2 inhibition assay. The inhibitory effects of all DCZ0358 derivatives on hCE2 were investigated using fluorescein diacetate (FD) as a specific probe substrate,[40] while LPA was used as a positive inhibitor of hCE2 in this study.[41] In brief, 200 μL incubation mixture containing 0.1 M PBS (PH = 7.4), human liver microsomes (2 μg mL^{-1}, final concentration) and each inhibitor. After 10 min pre-incubation at 37 °C, the reaction was initiated by adding FD (5 μM, final concentration, close to the K_m value of FD in HLM). After incubating for 30 min at 37 °C in a shaking bath, the reaction was stopped by the addition of acetonitrile (200 μL). The chemical structure of FD and its hydrolytic metabolite (fluorescein), as well as the detection conditions for fluorescein are depicted in Table S1.† The negative control incubation (DMSO only) was also carried out under the same conditions.[42] The residual activity was calculated using the formula mentioned above in hCE1 inhibition assay. The residual activities are shown in Fig. S1.†

Cell culture and fluorescence imaging analyses. In view of that hCE2 was an intracellular enzyme, the inhibition potential of **23o** was investigated in living HepG2 cells. The HepG2 cells were cultured in Modified Eagle's Medium (MEM) with 5% CO_2 and 0.1% antibiotic–antimycoticmix antibiotic at 37 °C, supplemented with 10% fetal bovine serum (FBS) and used NCEN as substrate probe to assay the **23o** inhibition potential toward hCE2. NCEN,[43] another specific optical probe substrate for hCE2, the structure and hydrolytic site were shown in Fig. S2(A).†

For fluorescence imaging, HepG2 cells were seeded in 96-well plates (8000 cells per well) with complete medium and then incubated for 24 hours. Afterwards, the cells were washed twice with FBS-free culture medium and then preincubated in the medium containing **23o** (prepared in FBS-free at various concentrations) for 30 min with 5% CO_2 at 37 °C. HepG2 cells were then co-incubated with NCEN (final concentration, 10 μM) for another 50 min to assess the intracellular hCE2 function, respectively. The living cells were imaged and analyzed using an ImageXpress® Micro Confocal High-Content Imaging system (Molecular Devices, Austria).

Conflicts of interest

There are no conflicts to declare.

Acknowledgements

We are grateful to Xiaolong Li and Hui Li for their early exploration of synthesizing this type of quaternary ammonium. This research was supported by grants from the National Key R & D Program of China (2016YFA0502301, 2017YFC1700200, 2017YFC1702000), National Major Scientific and Technological Special Project for "Significant New Drugs Development" (2018ZX09711002), National Natural Science Foundation of China (81573350, 81273546, 81973286, 8192207), Natural Science Foundation of Shanghai, China (19ZR1467800), and Program of Shanghai Academic/Technology Research Leader (18XD1403600).

Notes and references

1 L. W. Zou, Q. Jin, D. D. Wang, Q. K. Qian, D. C. Hao, G. B. Ge and L. Yang, *Curr. Med. Chem.*, 2018, **25**, 1627–1649.
2 D. D. Wang, L. W. Zou, Q. Jin, J. Hou, G. B. Ge and L. Yang, *Fitoterapia*, 2017, **117**, 84–95.
3 D. D. Wang, L. W. Zou, Q. Jin, J. Hou, G. B. Ge and L. Yang, *Acta Pharm. Sin. B*, 2018, **8**, 699–712.
4 P. M. Potter, J. S. Wolverton, C. L. Morton, M. Wierdl and M. K. Danks, *Cancer Res.*, 1998, **58**, 3627–3632.
5 S. P. Sanghani, S. K. Quinney, T. B. Fredenburg, W. I. Davis, D. J. Murry and W. F. Bosron, *Drug Metab. Dispos.*, 2004, **32**, 505–511.
6 E. T. Williams, K. O. Jones, G. D. Ponsler, S. M. Lowery, E. J. Perkins, S. A. Wrighton, K. J. Ruterbories, M. Kazui and N. A. Farid, *Drug Metab. Dispos.*, 2008, **36**, 1227–1232.
7 A. Watanabe, T. Fukami, M. Nakajima, M. Takamiya, Y. Aoki and T. Yokoi, *Drug Metab. Dispos.*, 2009, **37**, 1513–1520.
8 S. Chen, M. F. Yueh, C. Bigo, O. Barbier, K. Wang, M. Karin, N. Nguyen and R. H. Tukey, *Proc. Natl. Acad. Sci. U. S. A.*, 2013, **110**, 19143–19148.
9 R. H. Mathijssen, R. J. van Alphen, J. Verweij, W. J. Loos, K. Nooter, G. Stoter and A. Sparreboom, *Clin. Cancer Res.*, 2001, **7**, 2182–2194.
10 G. Dranitsaris, A. Shah, B. Spirovski and M. Vincent, *Clin. Colorectal Cancer*, 2007, **6**, 367–373.
11 S. K. Quinney, S. P. Sanghani, W. I. Davis, T. D. Hurley, Z. Sun, D. J. Murry and W. F. Bosron, *J. Pharmacol. Exp. Ther.*, 2005, **313**, 1011–1016.

12 A. Alimonti, A. Gelibter, I. Pavese, F. Satta, F. Cognetti, G. Ferretti, D. Rasio, A. Vecchione and M. Di Palma, *Cancer Treat. Rev.*, 2004, **30**, 555–562.
13 Z. P. Mai, K. Zhou, G. B. Ge, C. Wang, X. K. Huo, P. P. Dong, S. Deng, B. J. Zhang, H. L. Zhang, S. S. Huang and X. C. Ma, *J. Nat. Prod.*, 2015, **78**, 2372–2380.
14 Z.-J. Zhang, X.-K. Huo, X.-G. Tian, L. Feng, J. Ning, X.-Y. Zhao, C.-P. Sun, C. Wang, S. Deng, B.-J. Zhang, H.-L. Zhang and Y. Liu, *RSC Adv.*, 2017, **7**, 28702–28710.
15 L. W. Zou, Y. G. Li, P. Wang, K. Zhou, J. Hou, Q. Jin, D. C. Hao, G. B. Ge and L. Yang, *Eur. J. Med. Chem.*, 2016, **112**, 280–288.
16 L. D. Hicks, J. L. Hyatt, S. Stoddard, L. Tsurkan, C. C. Edwards, R. M. Wadkins and P. M. Potter, *J. Med. Chem.*, 2009, **52**, 3742–3752.
17 M. J. Hatfield, L. G. Tsurkan, J. L. Hyatt, C. C. Edwards, A. Lemoff, C. Jeffries, B. Yan and P. M. Potter, *J. Nat. Prod.*, 2013, **76**, 36–44.
18 B. Li, G. Wang, Z. Xu, Y. Zhang, X. Huang, B. Zeng, K. Chen, J. Shi, H. Wang and W. Zhu, *Eur. J. Med. Chem.*, 2014, **77**, 204–210.
19 B. Li, S. Xue, Y. Yang, J. Feng, P. Liu, Y. Zhang, J. Zhu, Z. Xu, A. Hall, B. Zhao, J. Shi and W. Zhu, *Sci. Rep.*, 2017, **7**, 41287.
20 L. Gao, B. Li, G. Yang, P. Liu, X. Lan, S. Chang, Y. Tao, Z. Xu, B. Xie, X. Sun, Y. Wang, L. Hu, D. Yu, Y. Xie, W. Bu, X. Wu, W. Zhu and J. Shi, *Cancer Lett.*, 2018, **421**, 135–144.
21 B. Li, G. Wang, M. Yang, Z. Xu, B. Zeng, H. Wang, J. Shen, K. Chen and W. Zhu, *Eur. J. Med. Chem.*, 2013, **70**, 677–684.
22 F. Baur, D. Beattie, D. Beer, D. Bentley, M. Bradley, I. Bruce, S. J. Charlton, B. Cuenoud, R. Ernst, R. A. Fairhurst, B. Faller, D. Farr, T. Keller, J. R. Fozard, J. Fullerton, S. Garman, J. Hatto, C. Hayden, H. He, C. Howes, D. Janus, Z. Jiang, C. Lewis, F. Loeuillet-Ritzler, H. Moser, J. Reilly, A. Steward, D. Sykes, L. Tedaldi, A. Trifilieff, M. Tweed, S. Watson, E. Wissler and D. Wyss, *J. Med. Chem.*, 2010, **53**, 3675–3684.
23 S. R. Haadsma-Svensson, K. A. Cleek, D. M. Dinh, J. N. Duncan, C. L. Haber, R. M. Huff, M. E. Lajiness, N. F. Nichols, M. W. Smith, K. A. Svensson, M. J. Zaya, A. Carlsson and C. H. Lin, *J. Med. Chem.*, 2001, **44**, 4716–4732.
24 H. Franzyk, S. R. Jensen, C. E. Olsen and J. H. Rasmussen, *Nucleosides, Nucleotides Nucleic Acids*, 2002, **21**, 23–43.
25 E. L. Eliel, T. N. Ferdinand and S. M. Carolyn, *J. Org. Chem.*, 1954, **19**, 1693–1698.
26 D. S. Kashdan, J. A. Schwartz and H. Rapoport, *J. Org. Chem.*, 1982, **47**, 2638–2643.
27 J. M. Hook, L. N. Mander and R. Urech, *J. Org. Chem.*, 1984, **49**, 3250–3260.
28 M. Kondo, Y. Inoue, Y. Koeduka, M. Funahashi, A. Heya, N. Matsuo and N. Kawatsuki, *Chem. Lett.*, 2015, **44**, 1010–1012.
29 M. Cushman, A. Abbaspour and Y. P. Gupta, *J. Am. Chem. Soc.*, 1990, **112**, 5898.
30 K. Q. Ling, J. H. Ye, X. Y. Chen, D. J. Ma and J. H. Xu, *Tetrahedron*, 1999, **55**, 9185–9204.
31 S. Sundriyal, P. B. Chen, A. S. Lubin, G. A. Lueg, F. Li, A. J. P. White, N. A. Malmquist, M. Vedadi, A. Scherf and M. J. Fuchter, *MedChemComm*, 2017, **8**, 1069–1092.
32 M. Spulak, J. Pourova, M. Voprsalova, J. Mikusek, J. Kunes, J. Vacek, M. Ghavre, N. Gathergood and M. Pour, *Eur. J. Med. Chem.*, 2014, **74**, 65–72.
33 D. D. Wang, Q. Jin, L. W. Zou, J. Hou, X. Lv, W. Lei, H. L. Cheng, G. B. Ge and L. Yang, *Chem. Commun.*, 2016, **52**, 3183–3186.
34 J. Wang, E. T. Williams, J. Bourgea, Y. N. Wong and C. J. Patten, *Drug Metab. Dispos.*, 2011, **39**, 1329–1333.
35 Y. Q. Wang, Z. M. Weng, T. Y. Dou, J. Hou, D. D. Wang, L. L. Ding, L. W. Zou, Y. Yu, J. Chen, H. Tang and G. B. Ge, *Int. J. Biol. Macromol.*, 2018, **120**, 1944–1954.
36 D. Abigerges, J. P. Armand, G. G. Chabot, L. Da Costa, E. Fadel, C. Cote, P. Herait and D. Gandia, *J. Natl. Cancer Inst.*, 1994, **86**, 446–449.
37 D. D. Wang, Q. Jin, L. W. Zou, J. Hou, X. Lv, W. Lei, H. L. Cheng, G. B. Ge and L. Yang, *Chem. Commun.*, 2016, **52**, 3183–3186.
38 L. Feng, Z. M. Liu, J. Hou, X. Lv, J. Ning, G. B. Ge, J. N. Cui and L. Yang, *Biosens. Bioelectron.*, 2015, **65**, 9–15.
39 Y. Q. Wang, Z. M. Weng, T. Y. Dou, J. Hou, D. D. Wang, L. L. Ding, L. W. Zou, Y. Yu, J. Chen, H. Tang and G. B. Ge, *Int. J. Biol. Macromol.*, 2018, **120**, 1944–1954.
40 K. C. Leibman, *Drug Metab. Dispos.*, 1973, **1**, 487–488.
41 D. Abigerges, J. P. Armand, G. G. Chabot, L. Dacosta, E. Fadel, C. Cote, P. Herait and D. Gandia, *J. Natl. Cancer Inst.*, 1994, **86**, 446–449.
42 Z. M. Weng, G. B. Ge, T. Y. Dou, P. Wang, P. K. Liu, X. H. Tian, N. Qiao, Y. Yu, L. W. Zou, Q. Zhou, W. D. Zhang and J. Hou, *Bioorg. Chem.*, 2018, **77**, 320–329.
43 X. W. Cheng, X. Lv, H. Y. Qu, D. D. Li, M. M. Hu, W. Z. Guo, G. B. Ge and R. H. Dong, *Acta Pharm. Sin. B*, 2017, **7**, 657–664.